

A REVISED ESTIMATE OF PACIFIC-NORTH AMERICA MOTION AND IMPLICATIONS FOR WESTERN NORTH AMERICA PLATE BOUNDARY ZONE TECTONICS

Charles DeMets, Richard G. Gordon, Seth Stein, and Donald F. Argus

Department of Geological Sciences, Northwestern University

**Abstract.** For the past 20 years, much effort has been directed to determining the present-day relative motion of the Pacific and North American plates using two independent approaches. One uses geologic observations and geodetic measurements along the San Andreas Fault and other faults in the plate boundary zone. The other is based on plate motion models that incorporate spreading rates from marine magnetic anomalies, transform azimuths, and earthquake slip vectors. Geologic and geodetic studies find two principal elements of deformation: slip along the San Andreas of  $\sim 34$  mm/yr directed  $N41^\circ W$ , and extension across the Basin and Range province of about 10 mm/yr directed  $N56^\circ W$ . In contrast, plate motion studies find 56-60 mm/yr directed  $N35^\circ W$ . The discrepancy between these estimates, a vector of about 15 mm/yr oriented nearly due north, is often attributed to a combination of slip along faults parallel to the San Andreas and shortening normal to it. Here we revise the estimate of Pacific-North America motion by analyzing marine magnetic profiles from the Gulf of California. Since 3 Ma, spreading has averaged 48 mm/yr, 10 mm/yr slower than estimated before, and consistent with the 49 mm/yr spreading predicted by a new global plate motion model derived without any data along the Pacific-North America boundary. The discrepancy with geodetic and geologic estimates is thus reduced to only 5 mm/yr parallel to the San Andreas, 60% less than estimated before, and 7 mm/yr of shortening across the San Andreas, similar to prior estimates. These results suggest that strike-slip motion on faults west of the San Andreas is less than thought before, a conclusion consistent with geodetic, seismological, and other geologic observations.

Introduction

It has long been recognized [Atwater, 1970] that the  $\sim 60$  mm/yr rate of Pacific-North America motion inferred from marine magnetic anomalies in the Gulf of California (Figure 1) exceeds the geologically and geodetically determined San Andreas Fault slip rate of  $\sim 32-36$  mm/yr [Prescott et al., 1981; Sieh and Jahns, 1984]. Different estimates of the direction of Pacific-North America motion are also discordant: the San Andreas strikes  $N41^\circ W$ ,  $6^\circ$  counterclockwise of the direction predicted by the RM2 global plate motion model [Minster and Jordan, 1978]. These differences cannot be explained by extension across the Basin and Range province; addition of the observed  $\sim 10$  mm/yr extension oriented  $N56^\circ W$  reduces the rate difference but increases the azimuth difference [Minster and Jordan, 1984, 1987]. A vector of about 15 mm/yr oriented nearly due north, termed the *San Andreas discrepancy*, describes the difference between the relative motion vector from global plate motion models and that estimated from the sum of San Andreas and Basin and Range motion. The San Andreas discrepancy

measures how much Pacific-North America motion is taken up elsewhere in the plate boundary zone [Minster and Jordan, 1984, 1987; Weldon and Humphreys, 1986]. This motion, which is likely composed of a convergent component normal to the San Andreas and a strike-slip component parallel to the San Andreas, may occur at various locations, such as along the controversial San Gregorio-Hosgri fault system [Savage and Prescott, 1978; Gawthrop, 1978; Hanks, 1979]. Here we analyze all available plate motion data to improve estimates of Pacific-North America motion. We conclude that this motion is  $\sim 15\%$  slower and that the San Andreas discrepancy is smaller than previously thought.

Pacific-North America Motion

The only data available for directly measuring the Pacific-North America rate averaged over several m.y. are several magnetic profiles across the Gulf Rise, the spreading ridge north of the Tamayo transform in the southern Gulf of California (Figures 1 and 2). No correlatable magnetic anomalies have been found north of the Gulf Rise and magnetic profiles south of the Tamayo cannot be used because the oceanic lithosphere east of the East Pacific Rise may be part of the small Rivera plate, which moves independently of the North American plate [Atwater, 1970]. We have compiled and analyzed published and unpublished magnetic profiles crossing the Gulf Rise (Figure 2). The track-to-track correlation of peaks and troughs is good. The location of the ridge crest is poorly constrained by bathymetry [Kastens et al., 1979], but a well-defined short wavelength peak bisects the central anomaly: This central anomaly magnetic high and its flanking troughs are features of cen-

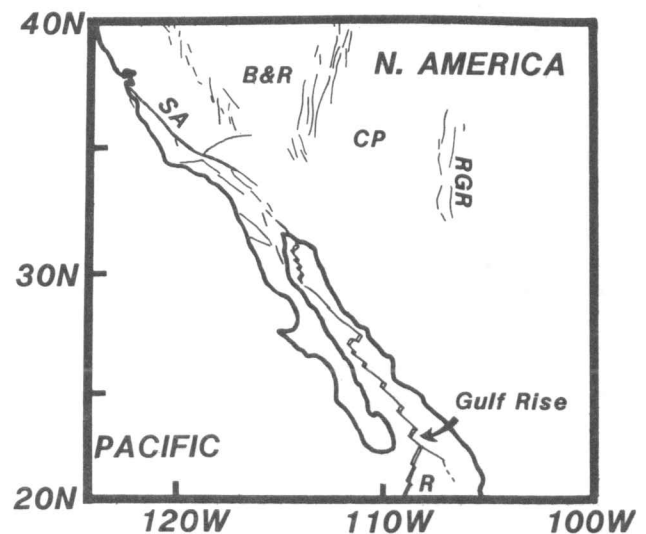


Fig. 1. Simplified tectonic map for the western U. S. and NE Pacific. SA=San Andreas Fault, CP=Colorado Plateau, RGR=Rio Grande Rift, R=Rivera Plate.

Copyright 1987 by the American Geophysical Union.

Paper number 7L7202.  
0094-8276/87/007L-7202\$03.00

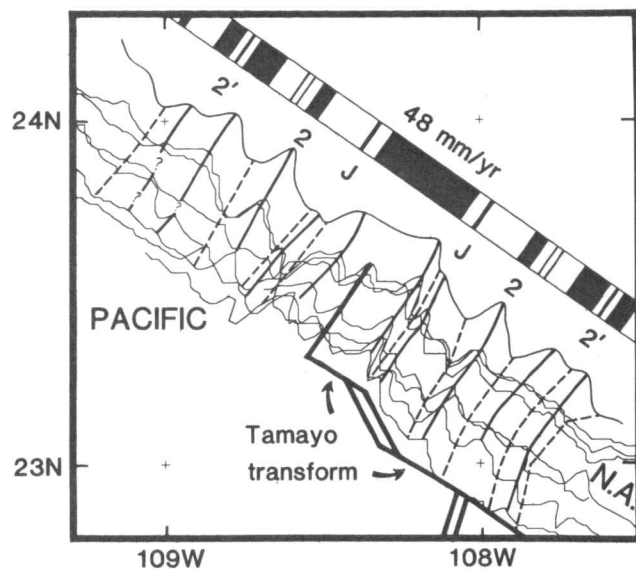


Fig. 2. Magnetic profiles across the Gulf Rise, the NE-trending ridge north of the Tamayo transform. From south to north, the profiles are GAM-2, GULFO-81, HYPO, MARSUR-78, HYPO, GAM-2, and GULFO-81. The northernmost satellite-navigated GULFO-81 profile has been translated  $\sim 6$  km SE and the southernmost HYPO profile has been translated  $\sim 5$  km NW along track into alignment with the other profiles for easy comparison. The magnetic anomalies in their original, untranslated positions suggest a small 5-10 km ridge offset between the GULFO-81 and MARSUR-78 ship-tracks. The synthetic magnetic anomaly assumes a constant 48 mm/yr spreading rate. Correlated peaks are connected by solid lines; correlated troughs are connected by dashed lines. We did not model the central anomaly magnetic high, which appears on the observed profiles as a peak bisecting the central anomaly. The synthetic, which uses a 1 km transition width out to anomaly 2 and a 3 km transition width for older anomalies, fits the shape and spacing of the observed anomalies 2 and 2'. A faster rate of  $\sim 51$  mm/yr would better fit the central and Jaramillo anomalies. The portion of the MARSUR-78 profile affected by a seamount, the Alarcon seamount, has been deleted here and in Figure 3.

tral anomalies world-wide. We have not modeled this magnetic high, which has been attributed to a narrow zone of strongly magnetized, recently extruded, unweathered basalt [Klitgord, 1976], but it provides a useful starting point for correlating the magnetic anomalies.

The Jaramillo anomaly (0.92-0.97 Ma according to the Harland et al. [1982] time scale, which is used throughout this paper) and anomaly 2 (1.67-1.87 Ma), the first large positive anomaly flanking the central anomaly, correspond well to the synthetic profile. On the SE flank a small correlatable peak appears east of the Jaramillo anomaly. Its origin is unclear but may be caused by a westward jump of the ridge crest at  $\sim 1$  Ma. Although the anomaly 2' sequence (2.48-3.40 Ma) is of low amplitude, on the SE flank a pair of peaks are correlatable from track to track. On the NW flank, the northern two tracks show two peaks that we correlate as the anomaly 2' sequence near where they are predicted by the synthetic. The anomaly 2' sequence on the southern four profiles is poorly defined. The lack of correlatable anomalies older than 2' is consistent with suggestions that sea-floor spreading began here  $\sim 4$  Ma [Larson et al.,

1968]. The 7 available profiles seem well-fit by a 48 mm/yr synthetic magnetic anomaly (Figures 2 and 3), but are poorly fit by the 58 mm/yr rate adopted by Larson et al. [1968], Atwater [1970], Minster and Jordan [1978], and Chase [1978]. Only about 20% of the difference in rate is caused by revisions in the reversal time scale over the past two decades. Figure 3, which shows five of the profiles reduced to the pole, illustrates the poor fit of a 58 mm/yr model. The width of the central anomaly and the separation of the Jaramillo anomalies suggest a faster ( $\sim 51$  mm/yr) spreading rate averaged since  $\sim 1$  Ma and the best-fit anomaly 2 average rate is 49 mm/yr. Here we focus on the 3 m.y. average, which is the standard for the NUVEL-1 global plate motion model (DeMets et al., ms. in preparation).

Comparison of the age-distance correlations of six of the profiles (Figure 4) shows some scatter about a constant spreading rate. The small scatter is consistent with random errors in the data, small ridge jumps, or minor variations in spreading rate since 3 Ma [cf. Vogt, 1986]. Prior estimates of 57-60 mm/yr for Gulf Rise spreading were based on the northern GAM-2 profile (Figures 2 and 3) [Larson et al., 1968; Atwater, 1970; Chase, 1978; Minster and Jordan, 1978]. Ness et al. [1985] have suggested a 65 mm/yr rate

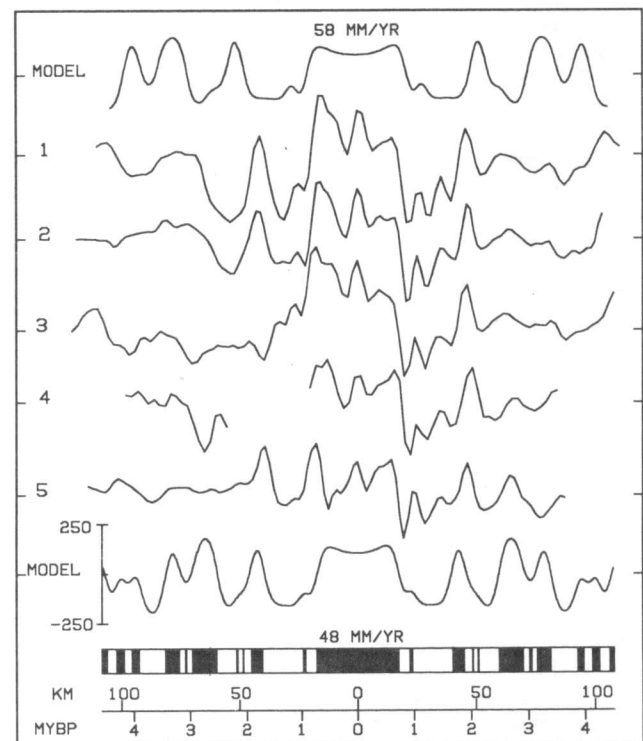


Fig. 3. Along-track (GULFO-81, GAM-2, and MARSUR-78) and projected (HYPO, N60°W) magnetic profiles are compared to 48 mm/yr and 58 mm/yr synthetic profiles. Profile 1 is the GULFO-81 north, #2 is the GAM-2 north, #3 is the HYPO north, #4 is the MARSUR-78, and #5 is the GULFO-81 south. All profiles have been reduced to the pole by a phase shift of  $83^\circ$  determined from the 1976 IGRF for the present field and an axial geocentric dipole model for the remanent magnetization. The profile-to-profile correlation of short and long wavelength features is good for the 48 mm/yr synthetic, but poor for the 58 mm/yr synthetic.

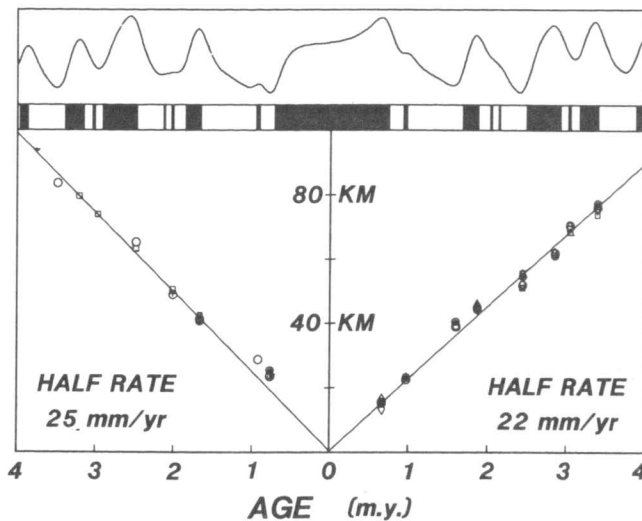


Fig. 4. Crustal age vs. distance from the ridge crest based on our magnetic anomaly correlations for six profiles labeled as follows: GAM-2 north="□"; GULFO-81 north="○"; HYPO north="◇"; MARSUR-78="△"; GULFO-81 south="●"; and HYPO south="+". Southeast is to the right. The best-fit average rate, derived by linear regression, is 47 mm/yr. The misfit of two 0.9 Ma correlations NW of the ridge axis suggests a slightly faster average rate since 0.9 Ma.

based on the northern GULFO-81 and the MARSUR-78 profiles. We have been unable to obtain a good fit to the data with either of these rates. Using all the data available, we find that a 48 mm/yr rate best fits the profiles to anomaly 2'.

Using the closures in a global relative plate motion model, Pacific-North America motion can be estimated without data from the Gulf of California. We deleted data along the entire Pacific-North America boundary and inverted the remaining NUVEL-1 global data to find a Pacific-North America Euler vector termed a *closure-fitting vector* [Minster and Jordan, 1984]. To be consistent with prior work, we treated Africa as a single plate. Our closure-fitting vector, a rotation of  $0.786^\circ/\text{m.y.}$  about a pole at  $46.5^\circ\text{N}$ ,  $75.4^\circ\text{W}$ , predicts  $49 \pm 3$  mm/yr spreading on the Gulf Rise, which agrees with the new magnetic anomaly rate.

#### The San Andreas Discrepancy

With the NUVEL-1 global plate motion dataset, which includes our revised Gulf Rise rate and up-to-date azimuthal data from the Gulf of California [Kastens et al., 1979; Niemitz and Bischoff, 1981; Goff et al., 1987], the Pacific-North America Euler vector is  $0.774^\circ/\text{m.y.}$  about a pole at  $48.4^\circ\text{N}$ ,  $76.5^\circ\text{W}$ . The lower Gulf Rise rate reduces, but does not eliminate, the San Andreas discrepancy. The linear velocity vector predicted by the NUVEL-1 Euler vector is larger than and rotated clockwise from the San Andreas vector, which parallels the fault trend in central California and is proportional to the observed  $\sim 34$  mm/yr slip rate (Figure 5). Although the new Euler vector predicts more fault-parallel motion than the summed San Andreas and Basin and Range vector, the discrepancy is less than found from RM2. The small ( $\sim 5$  mm/yr) fault-parallel discrepancy now predicted seems consistent with the low level of seismicity on the San Gregorio-Hosgri system and with geodetic measurements in the San Francisco area that

suggest little dextral slip west of the San Andreas [Prescott and Yu, 1986].

Although the fault-parallel discrepancy is less than found before, the fault-normal discrepancy is about the same as found before. The global vector predicts  $\sim 7$  mm/yr fault-normal shortening. Shortening has been suggested from independent geological data [Aydin and Page, 1984; Stein and King, 1984]. Crouch et al. [1984] summarize studies of post-Miocene ( $\sim 5.5$  Ma) convergence in central California and estimate a minimum 34 km of fault-normal shortening across the central California margin near the southern Hosgri Fault. The implied 6 mm/yr of shortening agrees with that predicted by our model, as does the geodetically determined  $6 \pm 2$  mm/yr shortening across part of the plate boundary zone in central California [Harris and Segall, 1987]. Harris and Segall [1987] note that the sense of shortening is consistent with orientations of fold axes and with thrust-faulting mechanisms within the plate boundary zone in central California.

The global vector is a compromise between the closure-fitting vector and the *best-fitting vector* (a rotation of

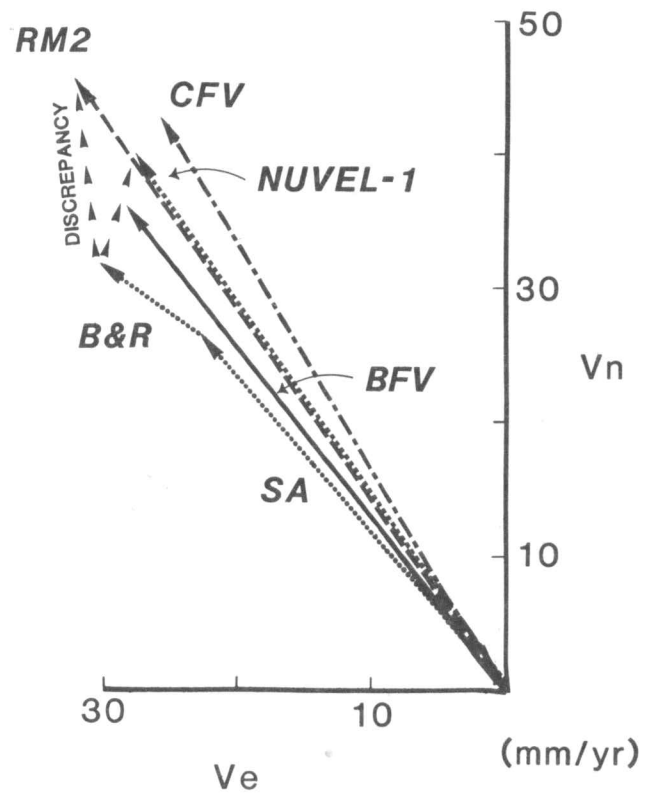


Fig. 5. Linear velocity vectors representing the observed and predicted relative motions at  $36^\circ\text{N}$  along the San Andreas Fault in central California. The predictions of the NUVEL-1 Pacific-North America best-fitting (BFV, solid), closure-fitting (CFV, alternating dashed), and global vector (NUVEL-1, thin solid) differ from the summed San Andreas and Basin and Range motion (dotted). The RM2 and NUVEL-1 discrepancy vectors are shown by lines of arrow heads. The fault-parallel component of the NUVEL-1 discrepancy vector is less than half that of RM2, whereas the fault-normal components of the two discrepancy vectors are similar. The predicted velocities from the global plate motion models of Minster and Jordan [1978] (long dashed) and Chase [1978] (not shown, 58 mm/yr,  $\text{N}35^\circ\text{W}$ ), are nearly identical.

0.708°/m.y. about a pole at 50.5°N, 74.5°W), which is found by inverting only data along the Pacific-North America boundary. In light of the many data analyzed, these two independent vectors are surprisingly different (Figure 5). Using an F-ratio test for plate circuit closure [Gordon et al., 1987], we find that the difference is significant at the 0.5% risk level. This difference has many possible explanations including systematic biases in the data, intra-plate deformation outside the assumed Pacific-North America plate boundary zone, or problems in combining 3 m.y.-average data (spreading rates) with instantaneous data (earthquake slip vectors). The discrepancy vector calculated from the closure-fitting vector predicts 6 mm/yr fault-parallel motion and 10 mm/yr fault-normal shortening, whereas the discrepancy vector calculated from the best-fitting vector predicts only 3 mm/yr fault-parallel motion and 4 mm/yr fault-normal shortening. If the difference between the best- and closure-fitting vectors is caused by a bias in the indirectly determined closure-fitting vector, then the San Andreas discrepancy may be even smaller than suggested by our global Euler vector. These questions might be resolved by local geodetic networks and space-based geodetic measurements from NASA's Crustal Dynamics Project.

**Acknowledgments.** We have benefitted from discussions with Gordon Ness, who first interested us in this problem, and with John Goff. We thank both for providing their data and ideas before publication. We also thank Bernard Minster, Tom Jordan, and Ross Stein for helpful comments. This research was supported by NSF grants EAR 8417323 and 8618038, and NASA Crustal Dynamics Contract NAG 5-885.

#### References

- Atwater, T., Implications of plate tectonics for the Cenozoic tectonic evolution of western North America, *Geol. Soc. Am. Bull.*, *81*, 3513-3536, 1970.
- Aydin, A., and B. M. Page, Diverse Pliocene-Quaternary tectonics in a transform environment, San Francisco Bay region, California, *Geol. Soc. Am. Bull.*, *95*, 1303-1317, 1984.
- Chase, C. G., Plate kinematics: The Americas, East Africa, and the rest of the world, *Earth Planet. Sci. Lett.*, *37*, 355-368, 1978.
- Crouch, J. K., S. B. Bachman, and J. T. Shay, Post-Miocene compressional tectonics along the central California margin, in *Tectonics and Sedimentation along the California Margin*, edited by J. K. Crouch and S. B. Bachman, pp. 37-54, S.E.P.M., Pacific Section, Fieldtrip Guidebook 38, 1984.
- Gawthrop, W. H., The 1927 Lompoc, California earthquake, *Bull. Seismol. Soc. Am.*, *68*, 1705-17167, 1978.
- Goff, J. A., E. A. Bergman, and S. C. Solomon, Earthquake source mechanisms and transform fault tectonics in the Gulf of California, *J. Geophys. Res.*, in press, 1987.
- Gordon, R. G., S. Stein, C. DeMets, and D. F. Argus, Tests of the closure of plate motion circuits, *Geophys. Res. Lett.*, *14*, 587-590, 1987.
- Hanks, T. C., The Lompoc, California earthquake (November 4, 1927;  $M=7.3$ ) and its aftershocks, *Bull. Seismol. Soc. Am.*, *69*, 451-462, 1979.
- Harland, W. B., A. V. Cox, P. G. Llewellyn, C. A. G. Pick-ton, A. G. Smith, and R. Walters, *A Geologic Time Scale*, 131 pp., Cambridge Univ. Press, New York, 1982.
- Harris, R. A., and P. Segall, Detection of a locked zone at depth on the Parkfield, California, segment of the San Andreas Fault, *J. Geophys. Res.*, *92*, 7945-7962, 1987.
- Kastens, K. A., K. C. Macdonald, and K. Becker, The Tamayo transform fault in the mouth of the Gulf of California, *Mar. Geophys. Res.*, *4*, 129-151, 1979.
- Klitgord, K. D., Sea-floor spreading: The central anomaly magnetization high, *Earth Planet. Sci. Lett.*, *29*, 201-209, 1976.
- Larson, R. L., H. W. Menard, and S. M. Smith, Gulf of California: a result of ocean-floor spreading and transform faulting, *Science*, *161*, 781-783, 1968.
- Minster, J. B., and T. H. Jordan, Present-day plate motions, *J. Geophys. Res.*, *83*, 5331-5354, 1978.
- Minster, J. B., and T. H. Jordan, Vector constraints on Quaternary deformation of the western United States east and west of the San Andreas Fault, in *Tectonics and Sedimentation along the California Margin*, edited by J. K. Crouch and S. B. Bachman, pp. 1-16, S.E.P.M., Pacific Section, Fieldtrip Guidebook 38, 1984.
- Minster, J. B., and T. H. Jordan, Vector constraints on western U. S. deformation from space geodesy, neotectonics and plate motions, *J. Geophys. Res.*, *92*, 4798-4804, 1987.
- Ness, G. E., M. W. Lyle, and A. T. Lonseth, Revised Pacific, North America, Rivera, and Cocos relative motion poles: Implications for strike-slip motion along the Trans-Mexican Volcanic Belt (abstract), *Eos Trans. AGU*, *66*, 849, 1985.
- Niemitz, J. W., and J. L. Bischoff, Tectonic elements of the southern part of the Gulf of California, *Geol. Soc. Am. Bull.*, *92 part II*, 360-407, 1981.
- Prescott, W. H., and S. Yu, Geodetic measurement of horizontal deformation in the northern San Francisco Bay region, California, *J. Geophys. Res.*, *91*, 7475-7484, 1986.
- Prescott, W. H., M. Lisowski, and J. C. Savage, Geodetic measurement of crustal deformation of the San Andreas, Hayward, and Calaveras faults near San Francisco, California, *J. Geophys. Res.*, *86*, 10,853-10,869, 1981.
- Savage, J. C., and Prescott, W. H., Geodetic control and the 1927 Lompoc, California earthquake, *Bull. Seismol. Soc. Am.*, *68*, 1699-1703, 1981.
- Sieh, K. E., and R. Jahns, Holocene activity of the San Andreas fault at Wallace Creek, California, *Geol. Soc. Am. Bull.*, *95*, 883-896, 1984.
- Stein, R. S., and G. C. P. King, Seismic potential revealed by surface folding: 1983 Coalinga, California, earthquake, *Science*, *224*, 869-872, 1984.
- Vogt, P. R., Plate kinematics during the last 20 m.y. and the problem of "present" motions, in *The Geology of North America, Volume M, The Western North Atlantic Region*, edited by P. R. Vogt and B. E. Tucholke, The Geological Society of America, Boulder, Col., 1986.
- Weldon, R., and E. Humphreys, A kinematic model of southern California, *Tectonics*, *5*, 33-48, 1986.

D. F. Argus, C. DeMets, R. G. Gordon, and S. Stein, Department of Geological Sciences, Northwestern University, Evanston, IL 60208

(Received June 24, 1987;  
accepted July 14, 1987.)